CYTOSKELETAL MOTORS

Myosin VI: an innovative motor that challenged the swinging lever arm hypothesis

James A. Spudich and Sivaraj Sivaramakrishnan

Abstract | The swinging crossbridge hypothesis states that energy from ATP hydrolysis is transduced to mechanical movement of the myosin head while bound to actin. The light chain-binding region of myosin is thought to act as a lever arm that amplifies movements near the catalytic site. This model has been challenged by findings that myosin VI takes larger steps along actin filaments than early interpretations of its structure seem to allow. We now know that myosin VI does indeed operate by an unusual ~ 180° lever arm swing and achieves its large step size using special structural features in its tail domain.

Molecular motors have key roles in virtually all cell biology processes. The precise, dynamic organization of cells and tissues depends crucially on these marvellous molecular machines. It is no wonder then that practically every cell has nearly 100 different molecular motors to carry out specific pivotal tasks. And, given the unique demands on the biochemical and biophysical properties of molecular motors to carry out their functions, they have given us a great deal of information about how enzymes work in general.

One such family of molecular motors is the myosin family. Myosins are ATPases that use the chemical energy derived from ATP hydrolysis to produce mechanical work. In 1969, H.E. Huxley[1] proposed the swinging crossbridge hypothesis to explain how this energy transduction might occur. According to current versions of this model, following ATP hydrolysis the myosin head domain (the crossbridge between the thick filament of myosin molecules and the thin actin filaments) undergoes a conformational transition into a pre-stroke state. On rebinding to actin and releasing phosphate, the ADP-bound myosin head undergoes a transition from a weak to a strong actin-binding state, which is accompanied by a reverse conformational change to a post-stroke state, resulting in a sliding motion at the actin–myosin interface. The myosin remains tightly bound to actin until ADP is released, at which point ATP rapidly binds and causes release of the myosin from actin. The fraction of the ATPase cycle time that a myosin spends strongly bound to an actin filament is known as the duty ratio. The strongly bound state time determines the maximum velocity of relative movement of myosin along an actin filament. The head cannot move forwards any faster than it can let go.

Crystal structures of several myosins[2–5] reveal that they are all composed of a catalytic head that binds to actin and nucleotides, with a converter domain distal to the actin-binding site (FIG. 1). The first myosin crystal structure identified a light chain-binding domain, which extends out from the myosin catalytic domain like a lever arm[6]. It has been assumed that for all myosins this light chain-binding region serves as a lever arm to amplify movements of the converter domain, which transitions between pre-stroke and post-stroke configurations (FIG. 1; light chains not shown). This transition is proposed to provide a mechanical stroke in a particular direction along the actin filament, which is a polar structure with barbed (also known as plus) and pointed (also known as minus) ends. Thus, the swinging crossbridge hypothesis was renamed the swinging lever arm hypothesis. What follows the light chain-binding domain varies between different myosins. Some myosins have a coiled-coil domain in this region, which is responsible for dimerization. Many have a cargo-binding domain at their carboxy terminus, which associates with specific cargo-binding proteins.

There are ~ 40 different myosin genes in higher eukaryotes[7], and each myosin carries out its own special functions *in vivo*. Muscle myosin (of the myosin II class), for example, is highly specialized to provide appropriate forces and velocities during muscle contraction[8]. A primary function of non-muscle myosin II is to drive cytokinesis[9]. Myosin I, myosin VI and myosin VII are

Department of Biochemistry, B400 Beckman Center, Stanford University School of Medicine, Stanford, California 94305-5307, USA. Correspondence to J.A.S. e-mail: jspudich@stanford.edu
doi:10.1038/nrm2833

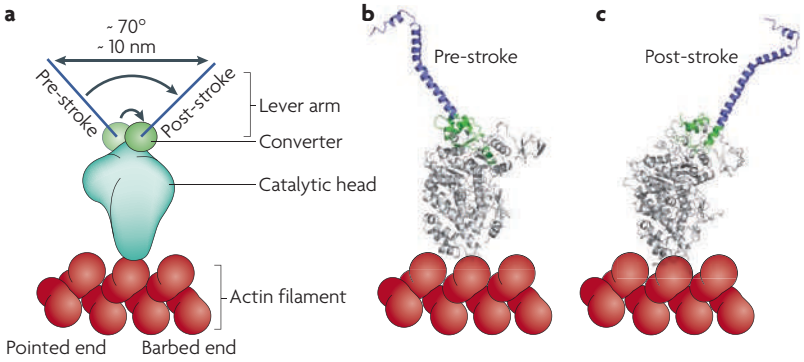

Figure 1 | **The swinging lever arm hypothesis.** Schematic (**a**) and crystal structures (**b**,**c**) of the myosin II head domain in pre-stroke and post-stroke states. The crystal structure of myosin is based on that of Rayment *et al.*[6] (protein data bank identifier 2MYS), with its lever arm extended on the basis of the structure obtained by Dominguez *et al.*[61] (protein data bank identifier 1BR2). All myosins are composed of a globular catalytic head domain, a converter and a lever arm. Conformational changes in the catalytic head are amplified by the lever arm during the ATPase cycle through an ~ 70° rotation of the converter. The lever arm of myosin II consists of an α-helix wrapped with two light chains (not shown here). The end of the lever arm is connected by the tail domains to a myosin thick filament in the case of myosin II, or to vesicular cargo in the case of the unconventional myosin V and myosin VI.

involved in the function of the inner ear, and mutations in them result in deafness[10]. Myosin V and myosin VI are involved in membrane trafficking and other aspects of cell organization. How all the different myosins are coordinated to carry out their various specialized tasks is an emerging field of research.

A particularly interesting member of the myosin family is myosin VI. Hasson *et al.*[11] identified mammalian myosin VI in a kidney proximal tubule cell line, in which it is localized to an apical actin-rich structure in epithelial cells called the brush border. The *Drosophila melanogaster* equivalent of myosin VI, 95F, had been implicated in the transport of cytosplasmic organelles[12,13]. Myosin VI is involved in various functions involving multiple cellular organelles (FIG. 2). For example, myosin VI localizes at the base of stereociliary bundles of hair cells (specialized filipodia) of the inner ear and is essential for their structural integrity[14]. Myosin VI at the cell periphery also has a role in border cell migration during development[15,16] and in cancer metastasis[17]. It is also involved in the transfer of endocytic vesicles from clathrin-coated pits to endosomes, along the cortical filamentous actin network. This includes the trafficking of rhodamine-labelled transferrin[18,19], cystic fibrosis transmembrane conductance regulator (CFTR)[20], lemur tyrosine kinase 2 (LMTK2; also known as BREK)[21,22] and α5β1 integrin[23]. Furthermore, myosin VI is recruited to the Golgi complex by optineurin[24], where it is essential for the maintenance of normal Golgi morphology[25]. How myosin VI carries out these diverse functions is unclear, although we do know some of the interacting proteins. These include disabled homologue 2 (DAB2)[26,27], GIPC1 (REF. 28), synapse-associated protein 97 (SAP97; also known as DLG1)[29] and optineurin[24], which have been found to target myosin VI to different cellular compartments.

Stereocilium
A tapered, finger-like projection from hair cells of the inner ear that responds to mechanical displacement with alterations in membrane potential, and thereby mediates sensory transduction.

Coiled coil
A protein structural domain that mediates subunit oligomerization. The most common coiled coil contains two α-helices that twist around each other to form a stable, rod-like structure.

Leucine zipper
A leucine-rich coiled-coil structural motif that is a common dimerization domain found in some proteins involved in regulating gene expression.

Similar to other myosins, myosin VI comprises a catalytic head with a converter domain, followed by light chain-binding domains (FIG. 2). The catalytic head is similar to that of myosin II and myosin V, with the exception of two inserts. One insert is near the nucleotide-binding pocket, which changes myosin VI's nucleotide kinetics relative to other myosins[4], and the second is an insert of 53 amino acids between the converter domain of the catalytic head and a canonical calmodulin-binding IQ motif[11,30]. This sequence is known as the unique insert (FIG. 3), and its C-terminal segment binds a single calmodulin[31]. The tail sequence beyond the calmodulin-binding region consists of the proximal tail, the medial tail, which is an unusual single α-helix (see below), and the cargo-binding domain[4,11,32] (FIG. 3).

When the primary sequence of myosin VI was first analysed, a major portion of its tail region seemed to be a coiled coil, similar to the tails of myosin II and myosin V. Because this motif is found in proteins that dimerize *in vivo*, it was assumed that this motor was a dimer. Nearly all *in vitro* studies have used a myosin VI construct truncated at Arg992 in the tail domain (near the end of the predicted coiled-coil region), followed by a strong coiled coil — the leucine zipper GCN4 motif — to ensure that the dimer does not dissociate at the low concentrations used for single molecule assays[33]. The ~ 300 residues at the C terminus that constitute the cargo-binding domain are absent in this myosin VI construct. We refer to this construct as an artificial dimer, as it was meant to be a substitute for a presumed native dimeric molecule involving interactions of the cargo-binding domain with its appropriate cargo. This artificial dimer has been useful to probe details of myosin VI behaviour; however, it is still unclear whether myosin VI functions as a dimer, a monomer or both *in vivo*.

Myosin VI moves along an actin filament in the opposite direction to all other myosins that have been characterized[30]. Myosin I[34], myosin II[35], myosin V[36], myosin X[37] and myosin XI[38] are directed towards the barbed ends of actin filaments. A truncated form of myosin IX was reported to move towards the pointed ends of actin filaments[39], but the native myosin IX molecule was subsequently shown to be a barbed end-directed motor[40]. Myosin VI moves towards the pointed ends of actin filaments, and this ability enables it to carry out specific functions *in vivo*. For example, the brush border of epithelial cells is polarized with the pointed ends of the actin filaments directed away from the plasma membrane[41]. This is consistent with roles for myosin VI in endocytosis[42] and myosin V in exocytosis[43]. Similarly, actin bundles in stereocilia are polarized such that myosin VI moves towards their base, thereby increasing membrane tension, which aids in stabilizing and maintaining appropriate tension in the stereocilia.

In addition to having reverse directionality, the artificial dimer of myosin VI has a larger step length on actin filaments than would be predicted from the early interpretations of the structure of the native protein, on the basis of current models of myosin movement[44,45]. These observations presented a serious challenge to the swinging lever arm hypothesis. In this Review, we discuss

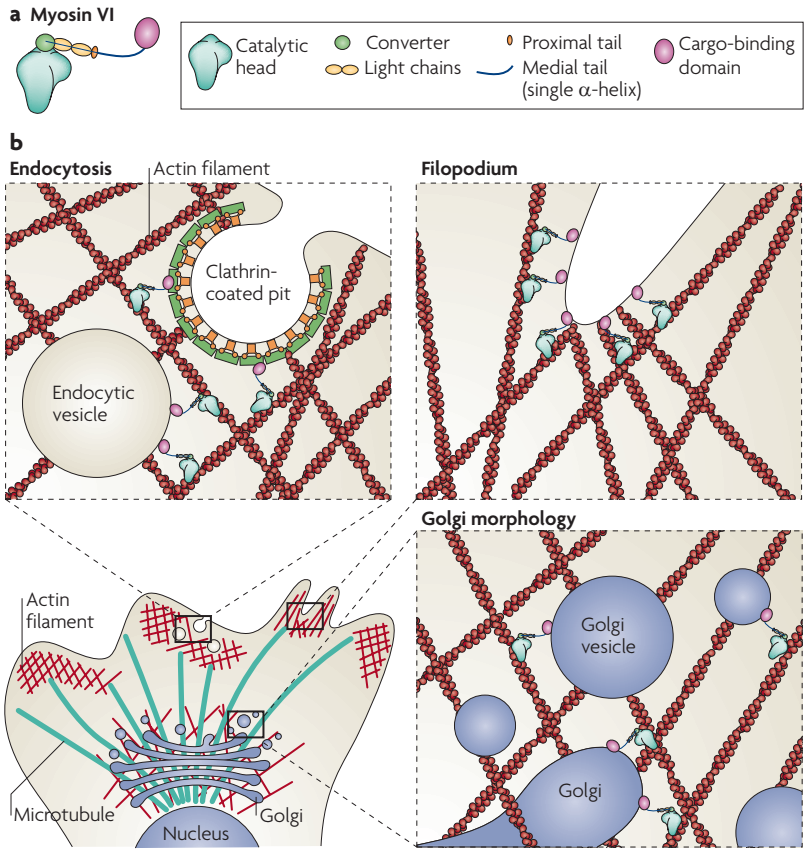

Figure 2 | **Schematic of myosin VI structure and some of its cellular functions.** **a** | Myosin VI consists of (sequentially from the amino terminus to the carboxy terminus) a catalytic head with a converter domain, two light chain-binding domains, a proximal tail, a medial tail and a cargo-binding domain (the distal tail (see REF. 32) has been incorporated into the cargo-binding domain here). **b** | Myosin VI has been implicated in several cellular processes, some of which are depicted here. For example, myosin VI is involved in the transfer of endocytic vesicles from clathrin-coated pits to endosomes along the cortical actin filament network. It is also found at the base of stereociliary bundles of hair cells (specialized filipodia) of the inner ear, where it is essential for their structural integrity, and has been found to have a role in maintaining normal Golgi morphology.

the results from *in vitro* motility assays, single molecule analysis, X-ray crystallography and other biophysical approaches, which proved pivotal in elucidating the unexpected, unique features of myosin VI with respect to its movement on actin filaments.

The swinging lever arm hypothesis

Huxley's swinging crossbridge model described above, now known as the swinging lever arm hypothesis, has been the favourite model used to explain how muscles contract and how non-muscle myosins function. However, since Huxley put the model forward in 1969 (REF. 1) there have been fascinating oscillations in its acceptance.

The swinging lever arm hypothesis under attack. Huxley's swinging crossbridge model of myosin movement on actin fell out of favour in the 1970s owing to a lack of support on several fronts. All biophysical studies that involved placing probes on a reactive cysteine in the myosin head failed to reveal conformational changes in the head domain (the crossbridge) as it transitioned from putative pre-stroke to post-stroke states[46,47]. Furthermore, the step size of myosin for each ATP used was frequently measured at > 100 nm[48], too large to be accounted for by a lever arm swing, which was unlikely to produce more than ~ 10 nm. These results led to the hypothesis that actin–myosin interactions are loosely coupled to ATP hydrolysis[48]. Furthermore, the movement of myosin on actin was proposed to be a result of Brownian motion of the myosin head together with preferential binding to a site on the actin filament in one direction (for example, towards the barbed end)[49]. This model of biased thermal diffusion is still prevalent in the current literature[49]. Indeed, it has been argued recently that biased thermal diffusion can explain the behaviour of processive myosin VI dimers[50], with intramolecular strain contributing to the directional bias during myosin stepping.

The swinging lever arm hypothesis revived. In the 1980s and 1990s, several developments paved the way for our current understanding of how myosins work. In 1984, single fluorescently labelled actin filaments were observed for the first time[51]. Subsequently, purified myosin II molecules bound to a microscope slide were shown to move fluorescently labelled purified actin filaments in the presence of ATP, at velocities comparable with those seen during muscle contraction[52]. Indeed, the myosin head domain was shown to be all that is needed for this *in vitro* motility[53]. This *in vitro* motility assay enabled the examination of small numbers of molecules interacting with an actin filament, under conditions in which many of the complexities of an intact muscle fibre were eliminated.

Given that the myosin head is the motor domain, the crystal structure constrains the lever arm stroke size to ~ 10 nm. However, step size estimates varied from ~ 10 nm[54–56] to > 100 nm[48,57,58]. These estimates were inferred from observations of multiple myosin molecules interacting with one or more actin filaments. It was therefore clear that a single myosin molecule going through a single cycle of interaction with actin had to be watched to directly measure its step size. Direct evidence for the predicted ~ 10 nm stroke for myosin II came from a single molecule optical trap study[59]. In the presence of ATP, myosin II was found to bind and almost instantaneously (< 1 ms) displace an actin filament by ~ 10 nm. This displacement in the optical trap is consistent with a swing of the end of the myosin lever arm of ~ 70°, resulting in a stroke size of ~ 10 nm. Subsequently, rigorous statistical methods, which form the current standard for the analysis of optical trapping data, confirmed a small step size for myosin[60].

These single molecule studies were consistent with later X-ray crystallography studies[61], in which a presumed pre-stroke crystal structure of myosin II bound to an ATP analogue was obtained. The lever was in a 'cocked' conformation, ~ 70° offset from the post-stroke structure[6], which was consistent with an ~ 10 nm displacement (FIG. 1). Since then, crystal structures of several myosins in different nucleotide analogue states have been

Brownian motion
The random, thermally driven motion of small objects in a fluid or gas.

Biased thermal diffusion
The random, thermally driven motion of a small object in a fluid, with a bias introduced by a localized attraction force.

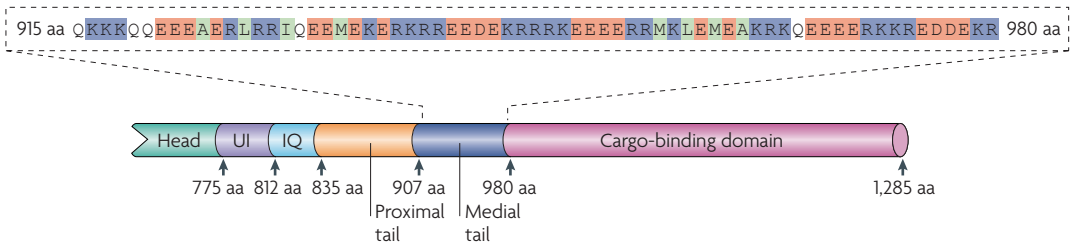

Figure 3 | **Schematic of the myosin VI lever arm and tail domains.** The amino acid numbers of the head, unique insert (UI), calmodulin-binding IQ motif, proximal tail, medial tail and cargo-binding domain of human myosin VI. The amino acid sequence of the ER/K motif-containing α-helix in the medial tail is shown in the expansion. The colours in this motif are used to depict the charge of the different amino acids based on standard CPK representation: positively charged amino acids (containing the primary amine and, therefore, nitrogen) are blue, negatively charged amino acids (containing an acid, for example oxygen) are orange and hydrophobic residues are green.

obtained, which have provided clues to how the myosin head moves to transduce the energy derived from ATP hydrolysis to the motion of the converter (FIG. 1), and consequently of the myosin lever arm. The inferred lever arm stroke from the crystal structures was confirmed by dynamic measurements using fluorescence resonance energy transfer[62,63].

Subsequently, the amplification of the stroke through the swing of the lever arm was also seen for myosin V[64,65]. This myosin is dimeric and has a high duty ratio, which renders it processive (that is, a single motor can move many steps along an actin filament without detaching)[36,66]. Myosin V has a large step size of ~ 36 nm; presumably a product of its long lever arm of six light chains, which extend beyond each catalytic domain, compared with muscle myosin, which binds only two light chains. Myosin V is arguably the best-studied molecular motor, and research on myosin V has provided strong support for the swinging lever arm model of myosin movement[67,68].

Myosin VI challenges the lever arm hypothesis

Despite strong support from extensive studies using myosin II and myosin V, the swinging lever arm hypothesis initially seemed to be inconsistent with the movement of myosin VI. Studies[45,44] found that artificial dimers of myosin VI are processive and have a large step size of ~ 36 nm. This step size was surprising because myosin VI has the same number of bound light chains as myosin II (FIG. 2), which could not support such a large step size on the basis of the ~ 70° lever arm swing predicted from studies of myosin II and myosin V. So how does myosin VI achieve such a large step size?

Myosin VI swings its lever arm domain ~ 180°. The first clues to how myosin VI steps along actin came from image reconstructions of cryo-electron micrographs with the myosin VI head domain bound to actin[30]. These showed that the light chain-binding region points in a direction opposite to that of myosin II in the presumed post-stroke state[30]. The crystal structure of the myosin VI head in the presumed post-stroke state[4] showed that the N-terminus of the unique insert wraps around the converter and forms an integral part of it (FIG. 4). This interaction redirects the myosin VI light chain-binding region in a direction opposite to that of myosin II and myosin V. This mechanical redirection was suggested to be the basis of the reversed direction of movement along actin, compared with that of other myosins[4].

To understand the role of the unique insert in myosin VI directionality, myosin VI constructs were created that were truncated after the IQ calmodulin-binding domain, after the unique insert calmodulin-binding domain, near the middle of the unique insert and directly after the converter[69]. Using *in vitro* motility and optical trap assays, the constructs truncated after the unique insert calmodulin-binding domain were found to move towards the pointed end of actin, whereas the construct truncated directly after the converter moved towards the barbed end of actin. This is consistent with the myosin head converter domain moving towards the barbed end of actin, as seen for myosin II and myosin V, with the end of the calmodulin-binding domain swinging around towards the pointed end. Thus, the shift in direction of myosin VI movement is clearly brought about by the unique insert domain. Others came to the same conclusion by showing that a myosin VI molecule truncated after the converter and fused to a myosin V lever arm moves towards the barbed end of actin filaments[70]. Importantly, the change in myosin VI stroke size as a function of the length of its lever arm was found to be consistent with a large (~ 180°) lever arm rotation from the pre-stroke to the post-stroke state[69] (FIG. 4). This finding was supported by the crystal structures of the myosin VI head in the pre-stroke and post-stroke states[4,5] (FIG. 4). Crystal structures revealed an unexpected, radical change in the arrangement of the α-helices in the converter domain in the myosin VI pre-stroke state[5] (FIG. 4). This new tertiary structure adopted by the converter explained the ability of this motor to swing its lever arm through this large angle. Other single molecule studies further confirmed this ~ 180° rotation[71,72]. The ~ 180° lever arm rotation seen for myosin VI results in a larger stroke than would have been predicted by the ~ 70° stroke that is characteristic of other myosins (FIG. 5), and these observations, together with the studies on myosin II and myosin V, provide overwhelming evidence in support of Huxley's swinging crossbridge hypothesis.

A fundamental issue, however, still remains. As already described, the step size of artificial myosin VI dimers has been measured at ~ 36 nm[44,73–75]. By contrast,

Stroke size
The distance travelled by the end of the lever arm of myosin following a single ATP hydrolysis. For a non-processive myosin, step size and stroke size are used interchangeably. For processive dimeric myosins, step size refers to the distance moved by the centre of mass of the molecule for a single ATP hydrolysis. Thus, for a processive dimer, the step size is the stroke size plus the additional distance the leading head travels by thermal diffusion before binding to actin.

Optical trap
An instrument that uses a focused laser beam to provide an attractive or repulsive force to physically hold and move microscopic dielectric objects.

Fluorescence resonance energy transfer
A process of energy transfer between two fluorophores. It can be used to determine the distance between two attachment positions in a macromolecule or between two molecules.

Small-angle X-ray scattering (SAXS). A system for nanostructure analysis in which nanosized particles scatter towards small angles. The SAXS pattern provides information on the overall size and shape of these particles.

Circular dichroism The differential absorption of left- and right-handed circularly polarized light. It is used to determine the secondary structure of proteins.

the stroke size of a single-headed construct of myosin VI truncated shortly after the calmodulin-binding domain (the canonical lever arm) is only ~ 12 nm[76], even with an ~ 180° swing. It must be emphasized that the step size of a processive dimeric motor can be longer than the stroke size of its lever arm, as an additional diffusive search by Brownian motion of the leading head of the dimer can result in its binding to an appropriately oriented actin monomer that is many nanometers in front[65,77]. However, the proposed tail structure of myosin VI could not support the additional 24 nm required to achieve a step size of 36 nm following an ~ 12 nm stroke, as described below.

The myosin VI tail domain allows the dimer to span ~ 36 nm along an actin filament. The IQ calmodulin-binding domain in myosin VI is followed by an ~ 70 amino acid sequence referred to as the proximal tail[32,76]. The proximal tail is followed by another ~ 70 amino acid sequence, termed the medial tail[32,78], which is strongly predicted by the algorithm PAIRCOILS[79] to be a coiled-coil domain[76]. A medial tail as a coiled coil would ensure that myosin VI is dimerized under certain cellular conditions. If the medial tail were a coiled coil, then the proximal tail would have to be an extensible, flexible element to allow the leading head to diffuse forwards the additional ~ 24 nm after the 12 nm stroke[45]. Indeed, disrupting the proximal tail by substituting a GCN4 leucine zipper coiled-coil motif into it abrogated the movement of myosin VI on actin filaments[76]. These findings supported a model in which the proximal tail is a flexible linker element that helps to span the ~ 24 nm gap in the myosin VI step.

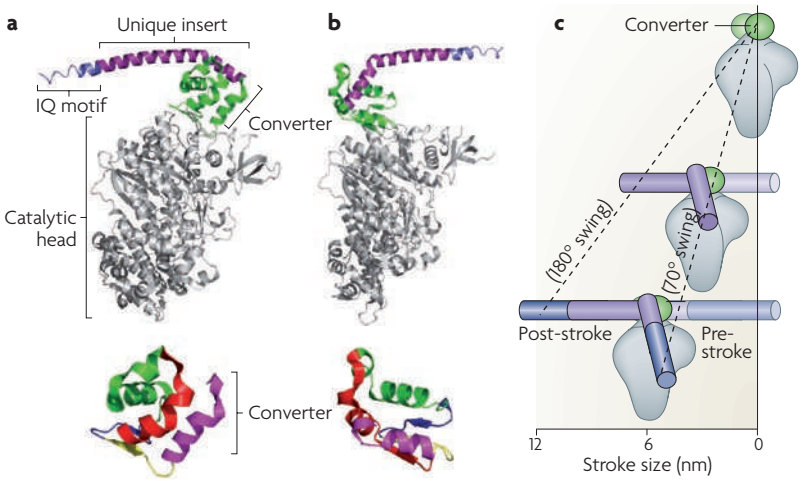

Figure 4 | **Reversing the direction of myosin VI.** The unique insert in the myosin VI lever arm changes the orientation of the lever arm as it emerges from the converter. **a** | Myosin VI in the post-stroke conformation[4] (protein data bank identifier 2BK1). **b** | Myosin VI in the pre-stroke conformation[5] (protein data bank identifier 2V26). The converter of myosin VI rotates ~ 180°, compared with ~ 70° in other myosins, resulting in an ~ 180° swing in the myosin VI lever arm from pre-stroke to post-stroke states. The blown up structures of the converters at the bottom of panels **a** and **b** show the change in the converter conformation between post-stroke and pre-stroke states. The individual α-helices and β-sheets are shown in different colours. **c** | The stroke size of myosin VI with one versus two light chain-binding domains, and swinging through 180° and 70°.

However, using small-angle X-ray scattering analyses, Spink *et al.*[32] suggested that the proximal tail in solution is a globular, folded domain of 2–3 nm in diameter and not an extended, flexible structure. The proximal tail was then shown to be a globular three-helix bundle by X-ray crystallography[80]. Thus, the proximal tail seemed most likely to be a structural element of myosin VI that might extend the lever arm, rather than acting as a flexible element to facilitate a large diffusive step.

So which tail structure could allow a dimeric myosin VI to straddle ~ 36 nm along an actin filament? When the strong coiled coil-forming GCN4 leucine zipper motif was inserted into the proximal region of the medial tail (presumed to be a coiled coil already), the myosin VI was unable to efficiently walk processively along an actin filament[32]. One explanation for this was that the medial tail is not a coiled coil at all. Consistent with this, a segment of the tail domain of myosin X, which was also predicted to be a coiled coil by the algorithm PAIRCOILS[79], was shown to be an isolated single α-helix in solution[81]. The authors pointed out that the medial tail of myosin VI has a similar, highly charged sequence and, therefore, may also be a single α-helix. Subsequent studies showed that this is indeed the case[78]. The isolated medial tail of myosin VI was found to have a high (> 90%) α-helical content[78], and measurements of its molecular weight in solution showed that it is monomeric in solution at concentrations as high as 40 μM[32]. Furthermore, when two copies of the medial tail were held in close proximity in solution through the formation of a disulphide bond between cysteines at the C-terminus of each monomer, no changes were seen in the melting profile in circular dichroism assays, in contrast to the sharp transition seen for canonical coiled coils[32]. Thus, the PAIRCOILS algorithm incorrectly predicts the medial tail to be a coiled coil because it assumes that a high density of charged residues, which make coiled coils soluble, is indicative of this structural motif. Indeed, for the most part, a heptad repeat pattern that is characteristic of coiled coils is not apparent in the medial tail. Low resolution reconstructions of the medial tail derived from small-angle X-ray scattering measurements clearly show an elongated structure that is consistent with the medial tail forming an isolated ~ 10 nm-long, single α-helix in solution[32]. Thus, it was suggested[32] that the simplest model of how myosin VI spans 36 nm along actin is that the two medial tail domains do not dimerize but each adds to the lever arm length; indeed, a monomeric construct of myosin VI that includes the medial tail shows a stroke size of 30 nm in the laser trap[78].

Although this model is satisfying in its apparent simplicity, Mukherjea *et al.*[80] presented data that relate back to a flexible proximal tail[76] and a dimerized medial tail. They proposed that even though the medial tail can be a single α-helix under some conditions, it has a weak dimerization site in its proximal region. They argued that dimerization only occurs when monomers of myosin VI are brought in close proximity, for example when concentrated on an actin filament[82]. The dissociation rate of these dimers, once formed, is fairly slow even after being released from actin. The authors showed by crystallography that the proximal tail domain is indeed a

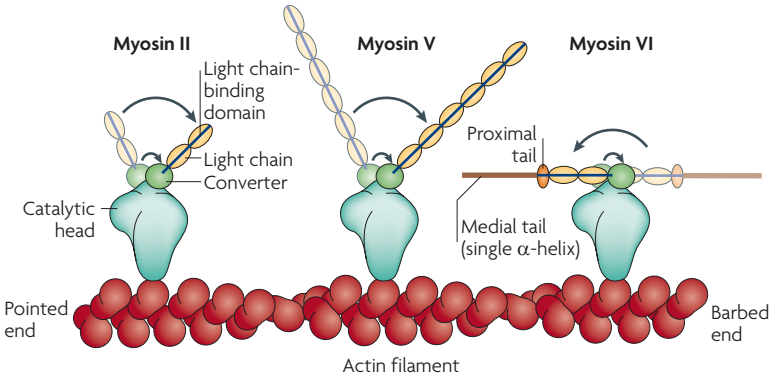

Figure 5 | **Schematic of lever arms in different myosins examined as single-headed species.** Myosin II has a short lever arm with two light chains bound that swings ~ 70°, resulting in an ~ 10 nm stroke (left). Myosin V has a longer lever arm with six light chains bound that also swings ~ 70°, resulting in an ~ 20 nm stroke (centre). Myosin VI has a lever arm with two light chains bound, a globular proximal tail and a single, rigid α-helix, all of which swing ~ 180°, resulting in a large stroke of ~ 30 nm (right).

three-helix bundle and provided evidence that it unfolds into a flexible element, maintaining three independently standing single α-helices. These findings only apply to myosin VI when dimerized. In this model, it is this flexible proximal tail domain that allows the dimeric myosin VI to span the 36 nm along actin.

One important difference between these two models is that the Spink *et al.* model proposes that myosin VI has a relatively rigid structure throughout its length, which allows it to step forwards with a normal step size even under backwards load. By contrast, myosin VI in the Mukherjea *et al.* model has a flexible proximal tail, and a marked reduction in step size would be predicted under backwards load. Laser trap studies with up to 2 pN backwards load have not detected an appreciable change in step size[83]. Although further experiments are needed to establish which of these models is correct, or indeed whether some combination of the two models is operating, it is clear that one or more of the tail domains beyond the calmodulin-binding domain is responsible for allowing the artificial dimer to span 36 nm along actin.

The ER/K motif-containing α-helix is an unexpected structural element. More studies are confirming that the medial tail can exist as a stable single α-helix in solution[78,84]. This is an unexpected finding, as protein α-helices are not generally considered to be stable in solution in the absence of the tertiary interactions found in folded proteins[85]. The sequence of the medial tail is homologous to two previously reported isolated, single, stable α-helices: a segment of the muscle protein caldesmon[86] and, as already mentioned, a region in the tail domain of myosin X[81]. The common feature of these α-helices is a repeating sequence of four negatively charged amino acids (glutamic acid (E)) followed by four positively charged amino acids (a combination of arginines (R) and lysines (K)), which we have termed the ER/K motif. Our studies[78] and bioinformatics analyses[84,87] have reported that the ER/K motif is present in various proteins from a range of species[84].

The stability of the medial tail ER/K motif-containing, single α-helix is a result of dynamic side chain charge–charge interactions between the E and R or K residues along the α-helical backbone[78] (FIG. 6a). We have measured the rigidity of this ER/K α-helix and have shown that it has a persistence length of ~ 15 nm[88]. This large persistence length is consistent with the medial tail in myosin VI, which contributes substantially to the stroke size of myosin VI (FIG. 6b), even in the presence of a large bending force in a dual beam optical trap assay[78], which would be expected to greatly reduce the step size of a more flexible element. Indeed, a monomeric construct of myosin VI that includes the medial tail gives a stroke size of ~ 30 nm[78]. It should be noted that the native (full length) myosin VI molecule has a stroke size of ~ 18 nm[89]. The reduced stroke size of the full length molecule is probably due to its folded state, with minimal stroke contribution from the medial tail[32,89].

We propose that the ER/K α-helix is a tensegrity structure that is stabilized by a balance between two sets of forces, namely those between the oppositely charged E and R/K side chains (tensile force) and the hydrogen bonds in the α-helical backbone (compressive force) (FIG. 6c). Tensegrity is a common design principle in nature[90] and sustains a range of biological structures, including the skeleton and the overall structure of the cellular cytoskeleton[91–93]. The stability of isolated α-helices is limited by interactions between polar water molecules and the hydrogen bonds in the backbone of the α-helix. The hydrogen bonds in the α-helical backbone are brittle and can tolerate little extension. Attack by a polar water molecule will destroy this interaction, causing the α-helix to unravel locally. In the ER/K α-helix, however, this is prevented by the long regions of hydrophobic residues on the side chains, which form a protective shell of hydrophobicity immediately surrounding the core of the α-helix[78]. Furthermore, the more malleable long-range charge–charge interactions between the E and R or K side chains enclose the backbone in the event of transient breaks in the backbone hydrogen bonds. Maintaining this α-helical conformation facilitates the formation of backbone hydrogen bonds and thereby stabilizes and strengthens this structure.

The swinging lever arm hypothesis is in good stead. The history of the swinging lever arm hypothesis shows how difficult it is to understand how any biological system really works. The myosin motor is one of the most studied enzymes and has seen several reversals in thinking about how it transforms the chemical energy of ATP hydrolysis into mechanical movement. The most recent challenge to the swinging lever arm hypothesis, the most popular model, was derived from the behaviour of myosin VI in single molecule experiments[44,45]. What was a great mystery a few years ago[44,45] can now be understood by a combination of a 180° swing of the myosin VI lever arm and one or another highly unusual tail domain that behaves in unexpected ways. Thus, the myosin that seemed as if it might disprove the hypothesis has corroborated it.

Persistence length
The length scale over which a structure is rigid.

Tensegrity
Short for tensional integrity. It refers to structures with an integrity that is based on a synergy between balanced tension and compression components.

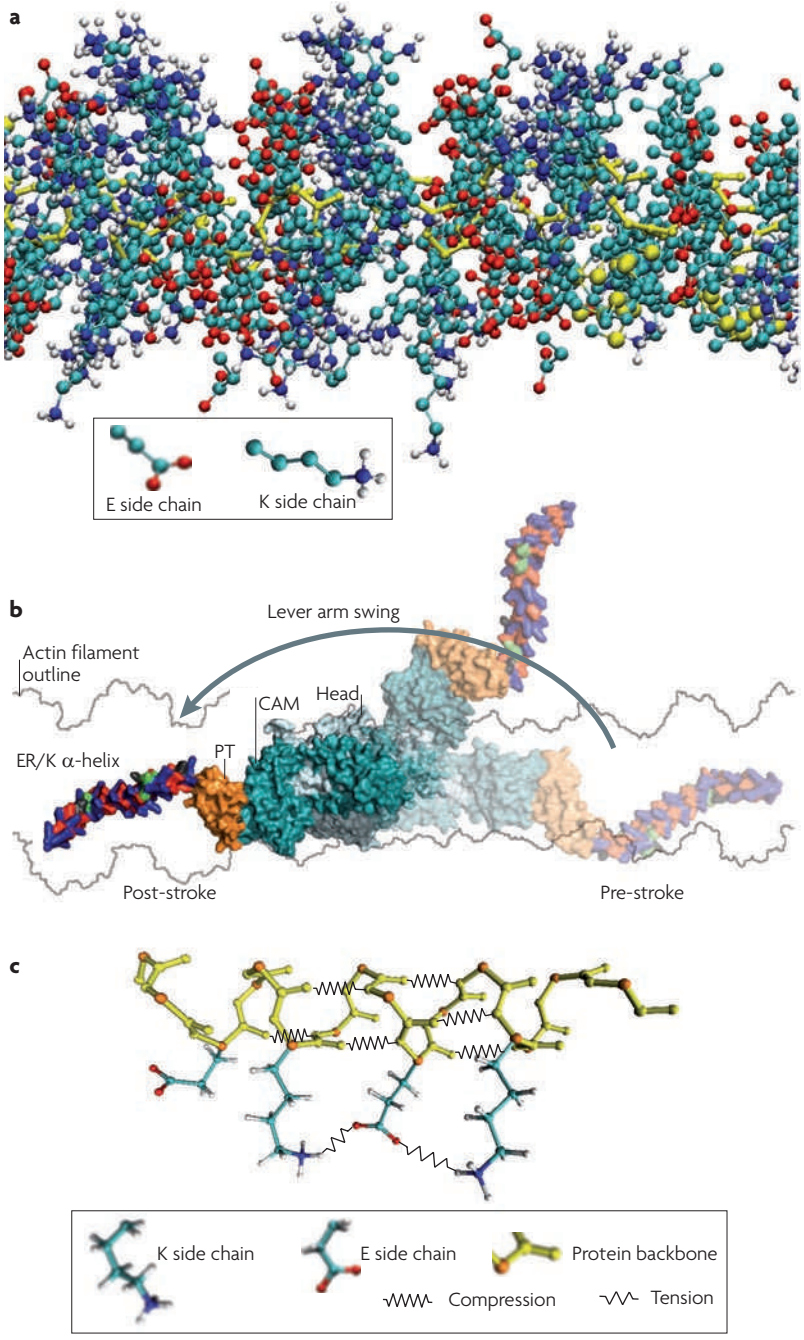

Figure 6 | **The ER/K motif-containing α-helix in the myosin VI lever arm.** **a** | Molecular dynamic simulations of the ER/K motif-containing α-helix in the medial tail of myosin VI show dynamic charge–charge interactions between the glutamic acid (E) and lysine (K) or arginine (R) residues. The colours used to depict the charge of the different amino acids are based on standard CPK representation. Positively charged amino acids (containing the primary amine and, therefore, nitrogen) are dark blue, and negatively charged amino acids (containing an acid, for example oxygen) are red. Carbon atoms in the side chains are green and hydrogen is white. **b** | Schematic of myosin VI showing the ~ 30 nm stroke that results from the rigid ER/K α-helix extension. The faded structures indicate the pre-stroke state as well as the movement of the lever arm until it reaches the post-stroke state. **c** | Our model of the ER/K motif-containing α-helix as a tensegrity structure[90,91]. The attractive forces between side chains can be considered to be under tension, whereas the CO–NH hydrogen bonds in the backbone can be considered to be under compression. The balance between these forces stabilizes the ER/K α-helix and enables it to withstand the bending forces that arise when the myosin VI lever arm strokes against an external load. PT, proximal tail.

Myosin VI function *in vivo*

In translating our understanding of myosin VI derived from *in vitro* experiments to its function *in vivo*, three pivotal questions need to be answered. First, how do mechanical forces in the molecule and mechanical forces that arise from interactions with other elements *in vivo* influence myosin VI function? Second, does myosin VI act as a dimer, a monomer or both *in vivo*? Finally, how do multiple myosins that are constrained to the same membrane compartment coordinate their movements *in vivo* to carry out their functions inside a cell?

Tension sensing and myosin VI processivity. An important concept to emerge from research on molecular motors is tension sensing to coordinate stepping, which is thought to be important for *in vivo* function. It is interesting that both myosin V and myosin VI give an ~ 25–30 nm stroke when the step size or stride of the dimeric molecules is ~ 36 nm. Why is this? This stroke can bring the trailing free head forwards, most of the way to its preferred actin binding site, but, importantly, not all the way there. Thermal energy would then be captured in a diffusion process, locking in intramolecular tension (arising between the two heads of the dimer) when the free head binds ~ 36 nm in front of the attached head. It is thought that the intramolecular tension between the two heads in the dimer when both heads are attached to actin allows them to have different nucleotide kinetics. In the case of myosin V, backwards force applied to the leading head reduces the ADP release rate[67,68]. Several kinetic measurements have been carried out to characterize the unique biochemical properties of the myosin VI motor domain as part of a monomer or the artificial dimer[33,94–96]. For the myosin VI artificial dimer, it has been proposed that it is the rate of ATP binding to the leading head that is reduced, rather than the rate of ADP release[95–97].

Similar to intramolecular tension sensing, intermolecular tension sensing can regulate motor activity. This type of regulation has been proposed for myosin VI, which is thought to act both as a transporter (for example, in the movement of endocytic vesicles) and as a structural anchor (to maintain the spatial organization of the Golgi complex)[83]. The motor is thought to be able to switch between these two functions by sensing external forces.

Much needs to be done to understand the roles of the different tail domains of myosin VI in transmitting loads through them to the catalytic site, thereby changing the behaviour of the motor. One approach is to replace parts of the tail with artificial protein structural domains, such as α-actinin repeats[98,99] or flexible linkers[98]. For example, myosin VI with α-actinin repeats replacing both the IQ domain and the proximal tail, and with a flexible linker between the α-actinin repeats and the medial tail, shows surprisingly robust processivity[98]. The effect of mechanical load on the behaviours of this construct, however, has yet to be examined.

***Coordinated function of myosin VI* in vivo.** Myosins that form native dimers and have a high duty ratio, such as myosin V, are processive *in vitro* and are highly likely to be dimers and to be processive *in vivo*[36]. Myosin VI,

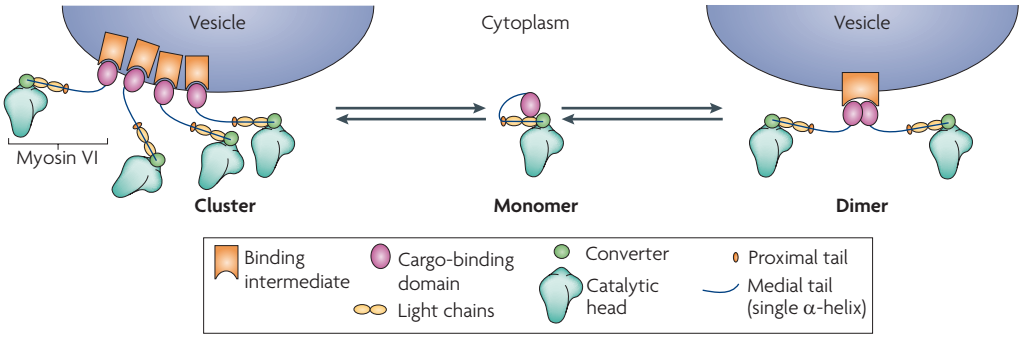

Figure 7 | **Myosin VI as a monomer and a dimer.** Myosin VI is a monomer when isolated from cells[89]. In the cytoplasm, the cargo-binding domain is probably folded back[32,89] and interacts with the head, with a potential regulatory function that has yet to be clarified. Myosin VI is depicted as a monomer in the cytoplasm (centre), as monomers that are part of clusters on a vesicle (left) or as a dimer on a vesicle (right). Although this schematic shows that the medial tail domains of myosin VI dimers do not interact, it has been suggested that the medial tail does in fact dimerize[80]. Clustering or dimerization on vesicles is probably mediated by adaptor proteins, which are bound to integral membrane proteins (together represented as a binding intermediate).

however, has been shown to be monomeric[89] when isolated in its native, full-length form. The myosin VI monomer seems to be a folded structure[32], suggesting that the cargo-binding domain interacts with the head domain, possibly with the lever arm itself (FIG. 7). It is possible that some unfolding of the proximal tail is necessary for the molecule to assume this folded configuration. As noted above, most studies on myosin VI stepping *in vitro* have forced dimerization by introducing a GCN4 leucine zipper coiled-coil motif at the end of the medial tail, ~ 290 residues from the C-terminus of the native protein[33]. If the medial tail is not a coiled coil, the effects are of dimerizing the motor artificially at this position and whether this motor ever functions as a dimer *in vivo* become open questions. Indeed, recent results show that four or more myosin VI monomers working together can transport nanoparticles long distances on a native cellular array of actin filaments[100] (FIG. 7). The number and oligomeric state of myosin VI molecules present on a given subcellular membrane compartment are not understood and need to be determined. If myosin VI functions as a monomer *in vivo*, the medial tail may be simply an extension of the canonical light chain-bound lever arm, and this would allow ~ 30 nm stroke sizes as the molecule moves forwards. If myosin VI were to function only as a monomer, then issues about the mechanisms by which dimers might function are not relevant.

What is missing and desperately needed at this point is a thorough biochemical and structural analysis of the interactions of myosin VI and its cargo-binding proteins, and a complete list of myosin VI binding partners[101]. Only when we understand the structures of entire native complexes of myosin VI bound to its cargoes can we properly begin to focus on how mechanical forces in the molecule and mechanical forces that arise from interactions with other elements *in vivo* influence myosin VI function, particularly how multiple myosins constrained to the same membrane compartment coordinate their movements *in vivo* to carry out their functions inside the cell.

In summary, much needs to be done to determine with certainty the oligomeric state of myosin VI as it functions *in vivo*. There is considerable circumstantial evidence supporting the idea that it can function as a dimer[32,80,82,102–105]. Indeed, GIPC and optineurin (which interact with myosin VI) are thought to be dimeric themselves and may therefore induce the dimerization of myosin VI[101]. However, if dimers are created by precise positioning of two monomers on a dimeric cargo[103], these dimers will clearly be structurally different from the experimental artificial dimer created by inserting a GCN4 motif near the end of the medial tail domain. The most important next step is to biochemically reconstitute the native myosin VI with its range of cargoes, allowing complete biochemical and biophysical characterization of such complexes. The feasibility of this approach has recently been shown[105].

Conclusions and perspectives

Understanding myosin VI function has been an important research focus over the past decade, fuelled by two unique characteristics of this myosin. The first is its ability to move along actin filaments in the opposite direction to all other myosins and the second is its ability to take large ~ 36 nm steps with what seemed at first to be a short lever arm. This represented a challenge to the swinging lever arm hypothesis. Both of these issues have now been largely resolved, and the swinging lever arm hypothesis has gained strong support.

The next big challenge for the field of molecular motors lies in translating detailed *in vitro* biochemical and biophysical characterizations into an understanding of motor function *in vivo*. Our knowledge of molecular motor function inside cells has been inferred primarily from the proteins or membrane compartments they associate with or from loss-of-function experiments *in vivo*. For instance, null myosin VI mutants lose the integrity of stereocilia, suggesting that myosin VI helps to generate membrane tension that stabilizes these structures. An important next step in bridging the gap

Molecular dynamic simulations
One of the principal tools in the theoretical study of biological molecules, which calculates the time-dependent behaviour of a molecular system.

between single molecule and other *in vitro* studies and *in vivo* function of motors such as myosin VI will be the thorough biochemical and structural characterization of the complexes made by these motors and their cargo-binding domains. Also needed is the development of new assays and techniques that facilitate the study of their coordinated function. Of particular interest will be understanding why the structure of myosin VI differs so much from other myosins and what purposes this design serves *in vivo*.

1. Huxley, H. E. The mechanism of muscular contraction. *Science* **164**, 1356–1365 (1969). **Proposes the swinging crossbridge hypothesis, which was later called the swinging lever arm hypothesis.**
2. Coureux, P. D., Sweeney, H. L. & Houdusse, A. Three myosin V structures delineate essential features of chemo-mechanical transduction. *EMBO J.* **23**, 4527–4537 (2004).
3. Himmel, D. M. *et al.* Crystallographic findings on the internally uncoupled and near-rigor states of myosin: further insights into the mechanics of the motor. *Proc. Natl Acad. Sci. USA* **99**, 12645–12650 (2002).
4. Menetrey, J. *et al.* The structure of the myosin VI motor reveals the mechanism of directionality reversal. *Nature* **435**, 779–785 (2005). **Presents the crystal structure of myosin VI in its post-stroke state, which reveals a redirection of the lever arm by the unique insert, first proposed here to be the source of the reverse directionality of this motor.**
5. Menetrey, J., Llinas, P., Mukherjea, M., Sweeney, H. L. & Houdusse, A. The structural basis for the large powerstroke of myosin VI. *Cell* **131**, 300–308 (2007). **Presents the crystal structure of myosin VI in its pre-stroke state, and reveals an unexpected change in conformation of the converter that allows a 180° rotation of the myosin VI lever arm.**
6. Rayment, I. *et al.* Three-dimensional structure of myosin subfragment-1: a molecular motor. *Science* **261**, 50–58 (1993).
7. Foth, B. J., Goedecke, M. C. & Soldati, D. New insights into myosin evolution and classification. *Proc. Natl Acad. Sci. USA* **103**, 3681–3686 (2006).
8. Bagshaw, C. *Muscle Contraction* (Chapman & Hall, London, 1993).
9. Burgess, D. R. Cytokinesis: new roles for myosin. *Curr. Biol.* **15**, R310–R311 (2005).
10. Redowicz, M. J. Myosins and pathology: genetics and biology. *Acta Biochim. Pol.* **49**, 789–804 (2002).
11. Hasson, T. & Mooseker, M. S. Porcine myosin-VI: characterization of a new mammalian unconventional myosin. *J. Cell Biol.* **127**, 425–440 (1994).
12. Kellerman, K. A. & Miller, K. G. An unconventional myosin heavy chain gene from *Drosophila melanogaster*. *J. Cell Biol.* **119**, 823–834 (1992).
13. Mermall, V., McNally, J. G. & Miller, K. G. Transport of cytoplasmic particles catalysed by an unconventional myosin in living *Drosophila* embryos. *Nature* **369**, 560–562 (1994).
14. Avraham, K. B. *et al.* The mouse Snell's waltzer deafness gene encodes an unconventional myosin required for structural integrity of inner ear hair cells. *Nature Genet.* **11**, 369–375 (1995).
15. Geisbrecht, E. R. & Montell, D. J. Myosin VI is required for E-cadherin-mediated border cell migration. *Nature Cell Biol.* **4**, 616–620 (2002).
16. Yoshida, H. *et al.* Lessons from border cell migration in the *Drosophila* ovary: a role for myosin VI in dissemination of human ovarian cancer. *Proc. Natl Acad. Sci. USA* **101**, 8144–8149 (2004).
17. Dunn, T. A. *et al.* A novel role of myosin VI in human prostate cancer. *Am. J. Pathol.* **169**, 1843–1854 (2006).
18. Aschenbrenner, L., Naccache, S. N. & Hasson, T. Uncoated endocytic vesicles require the unconventional myosin, Myo6, for rapid transport through actin barriers. *Mol. Biol. Cell* **15**, 2253–2263 (2004).
19. Hasson, T. Myosin VI: two distinct roles in endocytosis. *J. Cell Sci.* **116**, 3453–3461 (2003).
20. Ameen, N. & Apodaca, G. Defective CFTR apical endocytosis and enterocyte brush border in myosin VI-deficient mice. *Traffic* **8**, 998–1006 (2007).
21. Chibalina, M. V., Seaman, M. N., Miller, C. C., Kendrick-Jones, J. & Buss, F. Myosin VI and its interacting protein LMTK2 regulate tubule formation and transport to the endocytic recycling compartment. *J. Cell Sci.* **120**, 4278–4288 (2007).
22. Inoue, T. *et al.* BREK/LMTK2 is a myosin VI-binding protein involved in endosomal membrane trafficking. *Genes Cells* **13**, 483–495 (2008).
23. Valdembri, D. *et al.* Neuropilin-1/GIPC1 signalling regulates α5β1 integrin traffic and function in endothelial cells. *PLoS Biol.* **7**, e25 (2009).
24. Sahlender, D. A. *et al.* Optineurin links myosin VI to the Golgi complex and is involved in Golgi organization and exocytosis. *J. Cell Biol.* **169**, 285–295 (2005).
25. Warner, C. L. *et al.* Loss of myosin VI reduces secretion and the size of the Golgi in fibroblasts from Snell's waltzer mice. *EMBO J.* **22**, 569–579 (2003).
26. Inoue, A., Sato, O., Homma, K. & Ikebe, M. DOC-2/DAB2 is the binding partner of myosin VI. *Biochem. Biophys. Res. Commun.* **292**, 300–307 (2002).
27. Morris, S. M. *et al.* Myosin VI binds to and localises with Dab2, potentially linking receptor-mediated endocytosis and the actin cytoskeleton. *Traffic* **3**, 331–341 (2002).
28. Naccache, S. N., Hasson, T. & Horowitz, A. Binding of internalized receptors to the PDZ domain of GIPC/synectin recruits myosin VI to endocytic vesicles. *Proc. Natl Acad. Sci. USA* **103**, 12735–12740 (2006).
29. Wu, H., Nash, J. E., Zamorano, P. & Garner, C. C. Interaction of SAP97 with minus-end-directed actin motor myosin, V. I. Implications for AMPA receptor trafficking. *J. Biol. Chem.* **277**, 30928–30934 (2002).
30. Wells, A. L. *et al.* Myosin VI is an actin-based motor that moves backwards. *Nature* **401**, 505–508 (1999).
31. Bahloul, A. *et al.* The unique insert in myosin VI is a structural calcium-calmodulin binding site. *Proc. Natl Acad. Sci. USA* **101**, 4787–4792 (2004).
32. Spink, B. J., Sivaramakrishnan, S., Lipfert, J., Doniach, S. & Spudich, J. A. Long single α-helical tail domains bridge the gap between structure and function of myosin VI. *Nature Struct. Mol. Biol.* **15**, 591–597 (2008). **Using various biophysical, biochemical and single molecule techniques to characterize structural elements in the tail domain of myosin VI, this study suggests a possible model that enables this motor to take large ~ 36 nm steps based on a 10 nm single α-helix domain.**
33. De La Cruz, E. M., Ostap, E. M. & Sweeney, H. L. Kinetic mechanism and regulation of myosin VI. *J. Biol. Chem.* **276**, 32373–32381 (2001).
34. Mooseker, M. S. & Coleman, T. R. The 110-kD protein-calmodulin complex of the intestinal microvillus (brush border myosin I) is a mechanoenzyme. *J. Cell Biol.* **108**, 2395–2400 (1989).
35. Huxley, H. E. Electron microscope studies on the structure of natural and synthetic protein filaments from striated muscle. *J. Mol. Biol.* **7**, 281–308 (1963).
36. Mehta, A. D. *et al.* Myosin-V is a processive actin-based motor. *Nature* **400**, 590–593 (1999).
37. Homma, K., Saito, J., Ikebe, R. & Ikebe, M. Motor function and regulation of myosin X. *J. Biol. Chem.* **276**, 34348–34354 (2001).
38. Tominaga, M. *et al.* Higher plant myosin XI moves processively on actin with 35 nm steps at high velocity. *EMBO J.* **22**, 1263–1272 (2003).
39. Inoue, A., Saito, J., Ikebe, R. & Ikebe, M. Myosin IXb is a single-headed minus-end-directed processive motor. *Nature Cell Biol.* **4**, 302–306 (2002).
40. O'Connell, C. B. & Mooseker, M. S. Native myosin-IXb is a plus- not a minus-end-directed motor. *Nature Cell Biol.* **5**, 171–172 (2003).
41. Mooseker, M. S. & Tilney, L. G. Organization of an actin filament-membrane complex. Filament polarity and membrane attachment in the microvilli of intestinal epithelial cells. *J. Cell Biol.* **67**, 725–743 (1975).
42. Aschenbrenner, L., Lee, T. & Hasson, T. Myo6 facilitates the translocation of endocytic vesicles from cell peripheries. *Mol. Biol. Cell* **14**, 2728–2743 (2003).
43. Eichler, T. W., Kogel, T., Bukoreshtliev, N. V. & Gerdes, H. H. The role of myosin Va in secretory granule trafficking and exocytosis. *Biochem. Soc. Trans.* **34**, 671–674 (2006).
44. Nishikawa, S. *et al.* Class VI myosin moves processively along actin filaments backward with large steps. *Biochem. Biophys. Res. Commun.* **290**, 311–317 (2002).
45. Rock, R. S. *et al.* Myosin VI is a processive motor with a large step size. *Proc. Natl Acad. Sci. USA* **98**, 13655–13659 (2001).
46. Cooke, R. The mechanism of muscle contraction. *CRC Crit. Rev. Biochem.* **21**, 53–118 (1986).
47. Cooke, R., Crowder, M. S., Wendt, C. H., Barnett, V. A. & Thomas, D. D. Muscle cross-bridges: do they rotate? *Adv. Exp. Med. Biol.* **170**, 413–427 (1984).
48. Yanagida, T. Loose coupling between chemical and mechanical reactions in actomyosin energy transduction. *Adv. Biophys.* **26**, 75–95 (1990).
49. Yanagida, T., Iwaki, M. & Ishii, Y. Single molecule measurements and molecular motors. *Philos. Trans. R. Soc. Lond., B, Biol. Sci.* **363**, 2123–2134 (2008).
50. Iwaki, M., Iwane, A. H., Shimokawa, T., Cooke, R. & Yanagida, T. Brownian search-and-catch mechanism for myosin-VI steps. *Nature Chem. Biol.* **5**, 403–405 (2009). **Proposes a model of myosin VI stepping based on a Brownian search-and-catch mechanism.**
51. Yanagida, T., Nakase, M., Nishiyama, K. & Oosawa, F. Direct observation of motion of single F-actin filaments in the presence of myosin. *Nature* **307**, 58–60 (1984).
52. Kron, S. J. & Spudich, J. A. Fluorescent actin filaments move on myosin fixed to a glass surface. *Proc. Natl Acad. Sci. USA* **83**, 6272–6276 (1986).
53. Toyoshima, Y. Y. *et al.* Myosin subfragment-1 is sufficient to move actin filaments *in vitro*. *Nature* **328**, 536–539 (1987).
54. Toyoshima, Y. Y., Kron, S. J. & Spudich, J. A. The myosin step size: measurement of the unit displacement per ATP hydrolysed in an *in vitro* assay. *Proc. Natl Acad. Sci. USA* **87**, 7130–7134 (1990).
55. Uyeda, T. Q., Kron, S. J. & Spudich, J. A. Myosin step size. Estimation from slow sliding movement of actin over low densities of heavy meromyosin. *J. Mol. Biol.* **214**, 699–710 (1990).
56. Uyeda, T. Q., Warrick, H. M., Kron, S. J. & Spudich, J. A. Quantized velocities at low myosin densities in an *in vitro* motility assay. *Nature* **352**, 307–311 (1991).
57. Harada, Y., Sakurada, K., Aoki, T., Thomas, D. D. & Yanagida, T. Mechanochemical coupling in actomyosin energy transduction studied by *in vitro* movement assay. *J. Mol. Biol.* **216**, 49–68 (1990).
58. Yanagida, T., Arata, T. & Oosawa, F. Sliding distance of actin filament induced by a myosin crossbridge during one ATP hydrolysis cycle. *Nature* **316**, 366–369 (1985).
59. Finer, J. T., Simmons, R. M. & Spudich, J. A. Single myosin molecule mechanics: piconewton forces and nanometre steps. *Nature* **368**, 113–119 (1994).
60. Molloy, J. E., Burns, J. E., Kendrick-Jones, J., Tregear, R. T. & White, D. C. Movement and force produced by a single myosin head. *Nature* **378**, 209–212 (1995).
61. Dominguez, R., Freyzon, Y., Trybus, K. M. & Cohen, C. Crystal structure of a vertebrate smooth muscle myosin motor domain and its complex with the essential light chain: visualization of the pre-power stroke state. *Cell* **94**, 559–571 (1998).
62. Yasunaga, T., Suzuki, Y., Ohkura, R., Sutoh, K. & Wakabayashi, T. ATP-induced transconformation of myosin revealed by determining three-dimensional positions of fluorophores from fluorescence energy transfer measurements. *J. Struct. Biol.* **132**, 6–18 (2000).
63. Shih, W. M., Gryczynski, Z., Lakowicz, J. R. & Spudich, J. A. A FRET-based sensor reveals large ATP hydrolysis-induced conformational changes and three distinct states of the molecular motor myosin. *Cell* **102**, 683–694 (2000).

64. Purcell, T. J., Morris, C., Spudich, J. A. & Sweeney, H. L. Role of the lever arm in the processive stepping of myosin, V. *Proc. Natl Acad. Sci. USA* **99**, 14159–14164 (2002).
65. Veigel, C., Wang, F., Bartoo, M. L., Sellers, J. R. & Molloy, J. E. The gated gait of the processive molecular motor, myosin, V. *Nature Cell Biol.* **4**, 59–65 (2002).
66. De La Cruz, E. M., Wells, A. L., Rosenfeld, S. S., Ostap, E. M. & Sweeney, H. L. The kinetic mechanism of myosin, V. *Proc. Natl Acad. Sci. USA* **96**, 13726–13731 (1999).
67. Sellers, J. R. & Veigel, C. Walking with myosin V. *Curr. Opin. Cell Biol.* **18**, 68–73 (2006).
68. Trybus, K. M. Myosin V from head to tail. *Cell. Mol. Life Sci.* **65**, 1378–1389 (2008).
69. Bryant, Z., Altman, D. & Spudich, J. A. The power stroke of myosin VI and the basis of reverse directionality. *Proc. Natl Acad. Sci. USA* **104**, 772–777 (2007).
Uses *in vitro* motility and single molecule optical trapping assays to reveal functional structural transitions in myosin VI, suggesting that myosin VI operates by a lever arm mechanism, that this lever arm swings a full 180° and that reverse directionality of myosin VI is determined by the unique insert.
70. Park, H. *et al.* The unique insert at the end of the myosin VI motor is the sole determinant of directionality. *Proc. Natl Acad. Sci. USA* **104**, 778–783 (2007).
Uses an *in vitro* motility total internal reflection assay using myosin VI–myosin V chimaeras to strongly suggest that reverse directionality of myosin VI is determined by the unique insert.
71. Sun, Y. *et al.* Myosin VI walks "wiggly" on actin with large and variable tilting. *Mol. Cell* **28**, 954–964 (2007).
72. Reifenberger, J. G. *et al.* Myosin VI undergoes a 180° power stroke implying an uncoupling of the front lever arm. *Proc. Natl Acad. Sci. USA* **106**, 18255–18260 (2009).
73. Iwaki, M. *et al.* Cargo-binding makes a wild-type single-headed myosin-VI move processively. *Biophys. J.* **90**, 3643–3652 (2006).
74. Okten, Z., Churchman, L. S., Rock, R. S. & Spudich, J. A. Myosin VI walks hand-over-hand along actin. *Nature Struct. Mol. Biol.* **11**, 884–887 (2004).
75. Yildiz, A. *et al.* Myosin VI steps via a hand-over-hand mechanism with its lever arm undergoing fluctuations when attached to actin. *J. Biol. Chem.* **279**, 37223–37226 (2004).
76. Rock, R. S. *et al.* A flexible domain is essential for the large step size and processivity of myosin VI. *Mol. Cell* **17**, 603–609 (2005).
77. Dunn, A. R. & Spudich, J. A. Dynamics of the unbound head during myosin V processive translocation. *Nature Struct. Mol. Biol.* **14**, 246–248 (2007).
78. Sivaramakrishnan, S., Spink, B. J., Sim, A. Y., Doniach, S. & Spudich, J. A. Dynamic charge interactions create surprising rigidity in the ER/K α-helical protein motif. *Proc. Natl Acad. Sci. USA* **105**, 13356–13361 (2008).
79. Berger, B. *et al.* Predicting coiled coils by use of pairwise residue correlations. *Proc. Natl Acad. Sci. USA* **92**, 8259–8263 (1995).
80. Mukherjea, M. *et al.* Myosin VI dimerization triggers an unfolding of a three-helix bundle in order to extend its reach. *Mol. Cell* **35**, 305–315 (2009).
Uses a combination of single molecule and biophysical techniques to suggest a model that enables myosin VI to take large ~ 36 nm steps, based on structural transitions in a three α-helix bundle in the myosin VI tail.
81. Knight, P. J. *et al.* The predicted coiled-coil domain of myosin 10 forms a novel elongated domain that lengthens the head. *J. Biol. Chem.* **280**, 34702–34708 (2005).
Provides strong evidence that a segment of the myosin X tail is not a coiled coil, as predicted, but a single α-helix.
82. Park, H. *et al.* Full-length myosin VI dimerizes and moves processively along actin filaments upon monomer clustering. *Mol. Cell* **21**, 331–336 (2006).
83. Altman, D., Sweeney, H. L. & Spudich, J. A. The mechanism of myosin VI translocation and its load-induced anchoring. *Cell* **116**, 737–749 (2004).
84. Suveges, D., Gaspari, Z., Toth, G. & Nyitray, L. Charged single α-helix: a versatile protein structural motif. *Proteins* **74**, 905–916 (2009).
85. Dill, K., Ozkan, S., Shell, M. & Weikl, T. The protein folding problem. *Annu. Rev. Biophys.* **37**, 289–316 (2008).
86. Wang, C. L. *et al.* A long helix from the central region of smooth muscle caldesmon. *J. Biol. Chem.* **266**, 13958–13963 (1991).
87. Peckham, M. & Knight, P. J. When a predicted coiled coil is really a single α-helix, in myosins and other proteins. *Soft Matter* **5**, 2493–2503 (2009).
88. Sivaramakrishnan, S. *et al.* Combining single molecule optical trapping and small angle X-ray scattering measurements to compute the persistence length of a protein ER/K α-helix. *Biophys. J.* **97**, 2993–2999 (2009).
89. Lister, I. *et al.* A monomeric myosin VI with a large working stroke. *EMBO J.* **23**, 1729–1738 (2004).
90. Ingber, D. The architecture of life. *Sci. Am.* **278**, 48–57 (1998).
91. Ingber, D. E. Tensegrity, I. Cell structure and hierarchical systems biology. *J. Cell Sci.* **116**, 1157–1173 (2003).
92. Haswell, E. S. Gravity perception: how plants stand up for themselves. *Curr. Biol.* **13**, R761–R763 (2003).
93. Kasza, K. E. *et al.* The cell as a material. *Curr. Opin. Cell Biol.* **19**, 101–107 (2007).
94. De La Cruz, E. M. & Ostap, E. M. Relating biochemistry and function in the myosin superfamily. *Curr. Opin. Cell Biol.* **16**, 61–67 (2004).
95. Oguchi, Y. *et al.* Load-dependent ADP binding to myosins V and VI: implications for subunit coordination and function. *Proc. Natl Acad. Sci. USA* **105**, 7714–7719 (2008).
96. Sweeney, H. L. *et al.* How myosin VI coordinates its heads during processive movement. *EMBO J.* **26**, 2682–2692 (2007).
97. Robblee, J. P., Cao, W., Henn, A., Hannemann, D. E. & De La Cruz, E. M. Thermodynamics of nucleotide binding to actomyosin V and VI: a positive heat capacity change accompanies strong ADP binding. *Biochemistry* **44**, 10238–10249 (2005).
98. Liao, J. C., Elting, M. W., Delp, S. L., Spudich, J. A. & Bryant, Z. Engineered myosin VI motors reveal minimal structural determinants of directionality and processivity. *J. Mol. Biol.* **392**, 862–867 (2009).
99. Manstein, D. J. Molecular engineering of myosin. *Philos. Trans. R. Soc. Lond., B, Biol. Sci.* **359**, 1907–1912 (2004).
100. Sivaramakrishnan, S. & Spudich, J. A. Coupled myosin VI motors facilitate unidirectional movement on an F-actin network. *J. Cell Biol.* **187**, 53–60 (2009).
101. Buss, F. & Kendrick-Jones, J. How are the cellular functions of myosin VI regulated within the cell? *Biochem. Biophys. Res. Commun.* **369**, 165–175 (2008).
102. Spudich, G. *et al.* Myosin VI targeting to clathrin-coated structures and dimerization is mediated by binding to Disabled-2 and PtdIns(4, 5)P2. *Nature Cell Biol.* **9**, 176–183 (2007).
Examines the structural motifs in the myosin VI cargo-binding domain, which mediate the attachment of myosin VI to membrane cargo.
103. Altman, D., Goswami, D., Hasson, T., Spudich, J. A. & Mayor, S. Precise positioning of myosin VI on endocytic vesicles *in vivo*. *PLoS Biol.* **5**, e210 (2007).
104. Yu, C. *et al.* Myosin VI undergoes cargo-mediated dimerization. *Cell* **138**, 537–548 (2009).
105. Phichith, D. *et al.* Cargo binding induces dimerization of myosin VI. *Proc. Natl Acad. Sci. USA* **106**, 17320–17324 (2009).

Acknowledgements
J.A.S is supported by grant GM33289 from the National Institutes of Health. S.S. is supported by an American Cancer Society postdoctoral fellowship.

Competing interests statement
The authors declare no competing financial interests.

DATABASES
Protein Data Bank: http://www.rcsb.org/pdb
1BR2 | 2BK1 | 2MYS | 2V26
UniProtKB: http://www.uniprot.org
CFTR | DAB2 | 95F | GIPC1 | LMTK2 | SAP97

FURTHER INFORMATION
James A. Spudich's homepage:
http://biochem.stanford.edu/spudich

ALL LINKS ARE ACTIVE IN THE ONLINE PDF